Iranian Journal of Numerical Analysis and Optimization
Vol. 7, No. 2, (2017), pp 15–37
DOI:10.22067/ijnao.v7i2.52085

Radial basis functions method for solving three-dimensional linear Fredholm integral equations on the cubic domains

M. Esmaeilbeigi*, F. Mirzaee and D. Moazami

Abstract

The main purpose of this article is to describe a numerical scheme for solving three-dimensional linear Fredholm integral equations of the second kind on the cubic domains. The method is based on interpolation by radial basis functions (RBFs) based on Gauss-Legendre nodes and weights. Error analysis is presented for this method. Finally, several examples are given and numerical examples are presented to demonstrate the validity and applicability of the method.

Keywords: Three-dimensional integral equation; Radial basis functions; Collocation method; Cubic domains.

1 Introduction

Consider the following three-dimensional linear Fredholm integral equation of the second kind

$$u(x,y,z) - \lambda \int_e^f \int_c^d \int_a^b K(x,y,z,r,s,t)u(r,s,t)drdsdt = h(x,y,z), (x,y,z) \in D, \quad (1)$$

*Corresponding author
Received 9 December 2015; revised 4 September 2016; accepted 16 November 2016
M. Esmaeilbeigi
Department of Mathematics, Faculty of Mathematical Sciences and Statistics, Malayer University, Malayer, Iran. e-mail: m.esmaeilbeigi@malayeru.ac.ir

F. Mirzaee
Department of Mathematics, Faculty of Mathematical Sciences and Statistics, Malayer University, Malayer, Iran. e-mail: f.mirzaee@malayeru.ac.ir

D. Moazami
Department of Mathematics, Faculty of Mathematical Sciences and Statistics, Malayer University, Malayer, Iran. e-mail: dmoazami@yahoo.com

where h and K are known functions, $u(x, y, z)$ is the unknown function to be determined, λ is a constant and D is an cubic domain.

Integral equations occur in a wide variety of physical applications. They are encountered in various fields of science and numerous applications such as: elasticity, plasticity, heat and mass transfer, oscillation theory, fluid dynamics, filtration theory, electrostatics, electrodynamics, game theory, control, queuing theory, electrical engineering, economics, medicine, etc. There are many different numerical methods for solving integral equations. Computational complexity of mathematical operations is the most important obstacle for solving integral equations in higher dimensions. The Nystrom method [15] and collocation method [5, 14, 29] are the most important approaches of the numerical solution of these integral equations.

To avoid the mesh generation, in recent years meshless techniques have attracted attention of researchers. In a meshless method, a set of scattered nodes are used instead of meshing the domain of the problem [6, 7, 26].

Among meshless methods, the radial basis functions (RBFs) method has become known as a powerful tool for the scattered data interpolation problem. The main advantage of radial basis functions is that they involve a single independent variable regardless of the dimension of the problem. One of the domain-type meshless methods, the so-called Kansa's method developed by Kansa in 1990 [20, 21], is obtained by directly collocating RBFs, particularly the multiquadric (MQ), for the numerical approximation of the solution. Kansa's method was recently extended to solve various ordinary and partial differential equations including the one-dimensional nonlinear Burgers equation [18] with shock wave, shallow water equations for tide and currents simulation [17], heat transfer problems [30], and free boundary problems [19, 23].

Furthermore, the RBFs have been applied on the one-dimensional domains for solving linear second kind Fredholm and Volterra integral equations in [12], linear integro-differential equations in [13], nonlinear Volterra-Fredholm-Hammerstein integral equations in [25] and systems of nonlinear integral equations in [11]. Also, a numerical solution of two-dimensional Fredholm integral equations of the second kind on the square domains by Gaussian radial basis functions without the error analysis is introduced in [1].

In this paper, we will use the radial basis functions (RBFs) approximation for solving three-dimensional linear Fredholm integral equations of the second kind on cubic domains. The remainder of the paper is organized as follows: in Section 2, we show that how the radial basis functions are used to approximate the solution. In Section 3, we present a numerical method for solving the linear Fredholm integral equations of the second kind by the RBF approximation. In Section 4, error analysis for the proposed method is presented. Numerical examples are given in Section 5. Finally, we conclude the article in Section 6.

2 An outline of RBFs

The radial basis function (RBF) method for multivariate approximation is one of the most often applied tools in modern approximation theory due to spectral accuracy, flexibility with respect to geometry, dimensional independence and ease of implementation especially when the task is to interpolate scattered data in multi dimensions. The multiquadric (MQ) method was originally introduced by Hardy in 1968 for the interpolation of two dimensional scattered data to solve a problem from cartography [16]. The problem was to construct a continuous function from a set of sparse, scattered measurements from some source points on a topographic surface, which exactly fit to the given data and provides a good approximation of the features of the surface such as location of hilltops, saddles, breaks in slope, and drainage junctions. In fact the MQ method is a special version of the radial basis functions method. In 1982 Franke tested a large number of interpolation methods for two dimensional scattered data, and found that MQ method was one of the most impressive [10].

Table 1: Some well-known functions that generate RBFs.

Name of function	Definition
Multiquadrics (MQ)	$\phi(\mathbf{x}) = \sqrt{\|\mathbf{x}\|_2^2 + c^2}$
Inverse multiquadrics (IMQ)	$\phi(\mathbf{x}) = \left(\sqrt{\|\mathbf{x}\|_2^2 + c^2}\right)^{-1}$
Inverse quartics (IQ)	$\phi(\mathbf{x}) = \left(\|\mathbf{x}\|_2^2 + c^2\right)^{-1}$
Gaussian (GA)	$\phi(\mathbf{x}) = \exp\left(-c\|\mathbf{x}\|_2^2\right)$
Thin plate splines (TPS)	$\phi(\mathbf{x}) = (-1)^{k+1}\|\mathbf{x}\|_2^{2k}\log\|\mathbf{x}\|_2$
Conical splines (CS)	$\phi(\mathbf{x}) = \|\mathbf{x}\|_2^{2k-1}$

Definition 1. [28] A function $\phi : \mathbb{R}^s \longrightarrow \mathbb{R}$ is called radial basis provided there exists a univariate function $\varphi : [0, \infty) \longrightarrow \mathbb{R}$ such that

$$\phi(\mathbf{x}) = \varphi(r),$$

where $r = \|\mathbf{x}\|$ and $\|.\|$ is some norm on $\mathbb{R}^s$, usually the Euclidean norm.

Some well-known RBFs are listed in Table 1. Plots of some RBFs are presented in Figure (1).

The idea of radial basis function method for interpolation is derived from piecewise polynomial interpolation using a function of Euclidean distance and defined as follows:

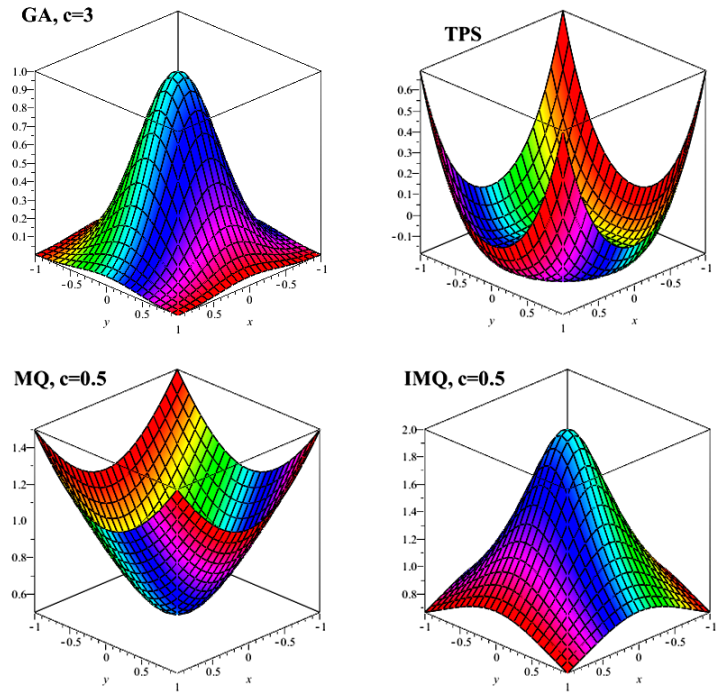

Figure 1: Plots of some radial basis functions.

2.1 Radial basis function interpolation

In the standard RBF interpolation problem, we are given generally scattered data sites $X = \{\mathbf{x}_1, \ldots, \mathbf{x}_N\} \subset D$ and associated real function values $u(\mathbf{x}_i), i = 1, \ldots, N$. Here D is usually some bounded domain in $\mathbb{R}^s$. It is our goal to find a (continuous) function $\mathscr{P}_N u : \mathbb{R}^s \to \mathbb{R}$ that interpolates the given data, i.e., such that

$$\mathscr{P}_N u(\mathbf{x}_i) = u(\mathbf{x}_i), \quad i = 1, \ldots, N. \tag{2}$$

In the RBF literature (see, e.g., [8, 28]) one assumes that this interpolant is of the form

$$\mathscr{P}_N u(\mathbf{x}) = \sum_{j=1}^{N} c_j \varphi\big(\|\mathbf{x} - \mathbf{x}_j\|\big), \tag{3}$$

where the basic function φ is assumed to be RBF and the coefficients $\mathbf{C} = [c_1, ..., c_N]^T$ are found by enforcing the interpolation constraints (2). This implies that

$$\mathbf{AC} = \mathbf{U}, \tag{4}$$

where $\mathbf{A}_{ij} = \varphi(\|\mathbf{x}_i - \mathbf{x}_j\|)$ and $\mathbf{U} = [u(\mathbf{x}_1), \ldots, u(\mathbf{x}_N)]^T$. If the matrix $\mathbf{A}$ is such that $\mathbf{C^T AC}$ is strictly positive for all possible choices of $X = \{\mathbf{x}_1, \ldots, \mathbf{x}_N\}$ and $\mathbf{C} = [c_1, ..., c_N]^T \in \mathbb{R}^N - \{0\}$ the solution of the interpolation problem is guaranteed.

The following results establish invertibility of the matrix A for different radial basis functions:

Definition 2. [28] A function ϕ is called completely monotone on $(0, \infty)$ if it satisfies $\phi \in C^\infty(0, \infty)$, and

$$(-1)^l \phi^{(-l)}(r) \geq 0,$$

for all $l \in \mathbb{N}_0$ and all $r > 0$. The function ϕ is called completely monotone on $[0, \infty)$ if it is in addition in $C[0, \infty)$.

Theorem 1. *[27] If $\phi(r) = \varphi(\sqrt{r})$ is completely monotone but not constant on $[0, \infty)$, then for any set of N distinct points $\{\mathbf{x}_1, \ldots, \mathbf{x}_N\}$, the $N \times N$ matrix $\mathbf{A}$ with entries $\varphi(\|\mathbf{x}_i - \mathbf{x}_j\|)$ is positive definite (and therefore non-singular).*

Theorem 2. *[24] Let $\phi(r) = \varphi(\sqrt{r}) \in C^0[0, \infty)$, $\phi(r) > 0$ for $r > 0$, $\phi'(r)$ completely monotone but not constant on $(0, \infty)$, then for any set of N distinct points $\{\mathbf{x}_1, \ldots, \mathbf{x}_N\}$, the $N \times N$ matrix $\mathbf{A}$ with entries $\varphi(\|\mathbf{x}_i - \mathbf{x}_j\|)$ is positive definite.*

It is easy to prove that the radial basis functions IMQ, IQ and GA satisfy the sufficient conditions of Theorem 1, whereas the MQ and linear RBFs satisfy the sufficient conditions of Theorem 2, and hence for these types of RBFs the system (4) is uniquely solvable for any set of distinct data points. Although the matrix $\mathbf{A}$ is non-singular in the above cases, usually it is very ill-conditioned. Therefore, a small perturbation in initial data may produce large amount of perturbation in the solution.

As given in Table 1, the types of RBF are mainly divided into two categories, infinitely smooth and piecewise smooth RBFs [2, 22]. The infinitely smooth RBFs contain a free parameter c, called the shape parameter, which affects both the accuracy of a solution and the conditioning of the collocation matrix. In Figure 2, a data set is interpolated with the Gaussian function, with different shape parameters. A smaller value of c causes the function to

become flatter, while increasing c leads to a more peaks RBF. The optimal value of the shape parameter that can produce relatively accurate results is to be found numerically. But the optimal choice of the shape parameters is an open problem which is still under intensive investigation. Several proposals for the choice of an adequate shape parameter can be found in the papers of Hardy [16], Franke [10] and Fasshauer [9]. All these proposals are somehow related with the number of points in the grid and the distance between those points.

Definition 3. Hardy's shape parameter

$$c = 0.815d \quad where \quad d = \frac{1}{N}\sum_{i=1}^{N} d_i,$$

where d_i is the distance from i^{th} center to the nearest neighbor and N is the total number of centers.

Definition 4. Franke's shape parameter

$$c = \frac{1.25D}{\sqrt{N}},$$

where D is the diameter of smallest circle encompassing all the center locations and N is the total number of centers.

Definition 5. Fasshauer's shape parameter

$$c = \frac{2}{\sqrt{N}},$$

where N is the total number of centers.

3 Solution of linear integral equations

In this paper, we solve the three-dimensional linear Fredholm integral equation given in the form

$$u(x,y,z) - \lambda \int_e^f \int_c^d \int_a^b K(x,y,z,r,s,t)u(r,s,t)drdsdt = h(x,y,z), (x,y,z) \in D, \quad (5)$$

where h and K are known functions, $u(x,y,z)$ is the unknown function to be determined, λ is a constant and D is an cubic domain.

Consider equation (5) with the following assumptions:

(i) $h \neq 0$ is continuous in $C(D)$,

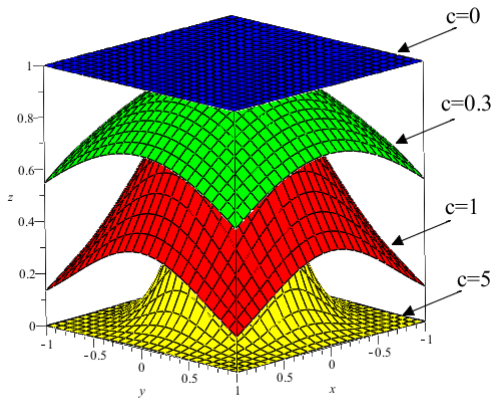

Figure 2: The Gaussian function, with different shape parameters, c.

(ii) K is continuous in $C(D \times D)$,

(iii) kernel $K(x, y, z, r, s, t)$ is real, continuous and bounded in the domain D, i.e.

$$L = \sup_{(x,y,z)\in D} \left\{ \int_e^f \int_c^d \int_a^b \left|K(x, y, z, r, s, t)\right| dr ds dt \right\} < \infty.$$

Theorem 3. *Existence and uniqueness of solution to equation (5) follow by assumptions* $(i) - (iii)$ *and the condition*

$$|\lambda| L < 1.$$

Proof. It can be proved using Banach's fixed point theorem in a similar method as done in [4], Chapter 5 (for one-dimensional linear Fredholm integral equations).

3.1 The proposed method

To apply the method, we need a RBF ϕ and N nodal scattered points to initiate the RBF method. These nodes can be selected arbitrary on the whole of the domain D, such as $X = \{(x_1, y_1, z_1), ..., (x_N, y_N, z_N)\}$. Therefore, to solve equation (5), we estimate the unknown function $u(x, y, z)$ by the RBF interpolation method as

$$u(x,y,z) \approx \sum_{k=1}^{N} \bar{c}_k \phi_k(x,y,z) = \bar{C}^T.\Psi(x,y,z), \qquad (x,y,z) \in D \subset \mathbb{R}^3, \quad (6)$$

where

$$\bar{C}^T = [\bar{c}_1, \ldots, \bar{c}_N],$$
$$\Psi^T(x,y,z) = [\phi_1(x,y,z), \ldots, \phi_N(x,y,z)],$$
$$\phi_k(x,y,z) = \varphi\Big(\sqrt{(x-x_k)^2 + (y-y_k)^2 + (z-z_k)^2}\Big), \qquad k = 1, \ldots, N.$$

We replace the expansion (6) with $u(x,y,z)$ and install the collocation points $(x_i, y_i, z_i), i = 1, 2, \ldots, N$ in equation (5). Thus we obtain

$$\bar{C}^T.\Big\{\Psi(x_i,y_i,z_i) - \lambda \int_e^f \int_c^d \int_a^b K(x_i,y_i,z_i,r,s,t)\Psi(r,s,t)drdsdt\Big\} = h(x_i,y_i,z_i). \quad (7)$$

The integrals in (7) must usually be evaluated numerically. we convert the intervals $[a,b], [c,d]$ and $[e,f]$ to the interval $[-1,1]$ by using a simple linear transformations of the form

$$\begin{cases} r = \dfrac{b-a}{2}\xi + \dfrac{b+a}{2} = g(\xi) \Longrightarrow dr = \dfrac{b-a}{2}d\xi, \\ s = \dfrac{d-c}{2}\eta + \dfrac{d+c}{2} = h(\eta) \Longrightarrow ds = \dfrac{d-c}{2}d\eta, \\ t = \dfrac{f-e}{2}\tau + \dfrac{f+e}{2} = m(\tau) \Longrightarrow dt = \dfrac{f-e}{2}d\tau, \end{cases}$$

and so equation (7) takes the following form:

$$\bar{C}^T.\Big\{\Psi(x_i,y_i,z_i) - \mu \int_{-1}^{1}\int_{-1}^{1}\int_{-1}^{1} K(x_i,y_i,z_i,g(\xi),h(\eta),m(\tau))\Psi(g(\xi),h(\eta),m(\tau))d\xi d\eta d\tau\Big\} = h(x_i,y_i,z_i), \quad (8)$$

where

$$\mu = \frac{\lambda(b-a)(d-c)(f-e)}{8}.$$

Using an m_N -point Gauss - Legendre quadrature formula with the points r_p, s_q, t_k in the interval $[-1,1]$ and weights w_p, w_q, w_k for numerical integration in equation (8), we can approximate the integral

$$\int_{-1}^{1}\int_{-1}^{1}\int_{-1}^{1} K(x,y,z,g(\xi),h(\eta),m(\tau))\Psi(g(\xi),h(\eta),m(\tau))d\xi d\eta d\tau, \qquad (9)$$

with

$$\sum_{p=1}^{m_N}\sum_{q=1}^{m_N}\sum_{k=1}^{m_N} w_p w_q w_k K(x,y,z,g(\xi_p),h(\eta_q),m(\tau_k))\Psi(g(\xi_p),h(\eta_q),m(\tau_k)). \tag{10}$$

Utilizing this numerical integration rule in equation (8), we obtain the following linear system of algebraic equations

$$\hat{C}^T.\Big\{\Psi(x_i,y_i,z_i)-\mu\sum_{p=1}^{m_N}\sum_{q=1}^{m_N}\sum_{k=1}^{m_N} w_p w_q w_k K(x_i,y_i,z_i,g(\xi_p),h(\eta_q),m(\tau_k))\Psi(g(\xi_p),h(\eta_q),m(\tau_k))\Big\} = h(x_i,y_i,z_i), \tag{11}$$

where $i = 1, 2, \ldots, N$. This is a linear system of equations that can be solved by iterative methods to obtain the unknown vector $\hat{C}^T$.

4 Error analysis

This section includes the error estimate and the rate of convergence of the presented method. To understand the numerical behavior of the interpolant or approximant it is essential to have bounds on the approximation error and on the condition number of the interpolation matrix. These bounds are usually expressed employing two different geometric measures. For the approximation error, it is crucial to know how well the data sites X fill the region . This can be measured by the fill distance

$$h_{_{X,D}} := \sup_{x\in D}\min_{1\le j\le N}\|\mathbf{x}-\mathbf{x}_j\|_2,$$

which gives the radius of the largest data-site free ball in D. The condition number, however, will obviously only depend on the data sites X and not on the region D. Moreover, if two data sites tend to coalesce then the corresponding interpolation matrix has two rows which are almost identical. Hence, it is reasonable to measure the condition number in terms of the separation distance

$$q_{_X} := \frac{1}{2}\min_{i\neq j}\|\mathbf{x}_i-\mathbf{x}_j\|.$$

A set X of data sites is said to be quasi-uniform with respect to a constant $c_{_{qu}} > 0$ if

$$q_{_X} \leqslant h_{_{X,D}} \leqslant c_{_{qu}} q_{_X}.$$

Definition 6. [28] The definition of the native space is

$$\aleph_\phi(D) = \left\{ f \in L_2(\mathbb{R}^s) \cap C(\mathbb{R}^s) : \frac{\hat{f}}{\sqrt{\hat{\phi}}} \in L_2(\mathbb{R}^s) \right\},$$

where $\hat{\phi}$ is a Fourier transform of ϕ.

Theorem 4. *[2] Let ϕ is positive definite RBF with infinitely smoothness. Suppose that $D \subset \mathbb{R}^s$ be open and bounded, satisfying an interior cone condition. Denote the interpolant of a function $u \in \aleph_\phi(D)$ based on this RBF and the distinct set $X = \{x_1, \ldots, x_N\}$ by $\mathscr{P}_{_N} u$. Then for every $l \in \mathbb{N}$ there exist constants $h_0(l), C_l$ such that*

$$\|u - \mathscr{P}_{_N} u\|_{L^\infty(D)} \leq C_l h^l_{_{X,D}} \|u\|_{\aleph_\phi(D)}, \tag{12}$$

for all $x \in D$, provided $h_{_{X,D}} \leqslant h_0(l)$.

Remark 1. As a conclusion from Theorem 4, for Gaussians $\phi(\mathbf{x}) = e^{(-c\|\mathbf{x}\|^2)}, c > 0$, we get for some positive constant l that

$$\|u - \mathscr{P}_{_N} u\|_{L^\infty(D)} \leq e^{\left(\frac{-l|\log h_{_{X,D}}|}{h_{_{X,D}}}\right)} \|u\|_{\aleph_\phi(D)}, \tag{13}$$

provided that $h_{_{X,D}}$ is sufficiently small and $u \in \aleph_\phi(D)$.

The corresponding result for (inverse) multiquadrics $\phi(\mathbf{x}) = (\|\mathbf{x}\| + c^2)^\alpha, c > 0, \alpha < 0$, or $\alpha > 0$ and $\alpha \neq \mathbb{N}$, is

$$\|u - \mathscr{P}_{_N} u\|_{L^\infty(D)} \leq e^{\left(\frac{-l}{h_{_{X,D}}}\right)} \|u\|_{\aleph_\phi(D)}, \tag{14}$$

For thin plate splines $\phi(\mathbf{x}) = (-1)^{k+1} \|\mathbf{x}\|^{2k} \log \|\mathbf{x}\|_2$, $k \in \mathbb{N}$, we get

$$\|u - \mathscr{P}_{_N} u\|_{L^\infty(D)} \leq C h^k_{_{X,D}} \|u\|_{\aleph_\phi(D)}. \tag{15}$$

Let $\mathscr{K}$ be the Urysohn integral operator:

$$(\mathscr{K} u)(x, y, z) = \lambda \int_e^f \int_c^d \int_a^b K(x, y, z, r, s, t) u(r, s, t) dr ds dt, \tag{16}$$

we can rewrite the integral equation (5) in operator form as

$$u - \mathscr{K} u = h. \tag{17}$$

Define the approximating operator $\mathscr{K}_N, N \geq 1$, on $C(D)$ by

$$\mathscr{K}_N u(x, y, z) = \mu \sum_{p=1}^{m_N} \sum_{q=1}^{m_N} \sum_{k=1}^{m_N} w_p w_q w_k K(x, y, z, g(\xi_p), h(\eta_q), m(\tau_k)) \hat{C}^T \Psi(g(\xi_p), h(\eta_q), m(\tau_k)). \tag{18}$$

The abstract form of equation (8) is

$$u_N - \mathscr{P}_{_N}\mathscr{K}u_N = \mathscr{P}_{_N}h,$$

for N sufficiently large and the above equation can be rewritten as

$$(I - \mathscr{P}_{_N}\mathscr{K})u_N = \mathscr{P}_{_N}h. \tag{19}$$

Remark 2. Note that, $\mathscr{P}_{_N} : C(D) \longrightarrow V_N$ is the collocation projection operator on the collocation points $X = \{(x_1, y_1, z_1), ..., (x_N, y_N, z_N)\} \subset D$, where the subspace $V_N := span\{\phi_1, \dots \phi_N\} \subset C(D)$ has finite dimension. Suppose $\hat{u} \in V_N$, we simply have $\mathscr{P}_{_N}\hat{u} = \hat{u}$.

The abstract form of equation (11) is

$$(I - \mathscr{P}_{_N}\mathscr{K}_N)\hat{u}_N = \mathscr{P}_{_N}h, \tag{20}$$

which shows that the scheme is a discrete collocation method [3].
Consequently an iterated discrete collocation solution can be obtained. For this purpose we set

$$\bar{u}_N = h + \mathscr{P}_{_N}\mathscr{K}_N(\hat{u}_N), \tag{21}$$

and by applying the operator $\mathscr{P}_{_N}$ on both sides of (21), and using the relation (20) we simply have

$$\mathscr{P}_{_N}\bar{u}_N = \hat{u}_N. \tag{22}$$

Thus we conclude

$$(I - \mathscr{P}_{_N}\mathscr{K}_N)\bar{u}_N = h. \tag{23}$$

Theorem 5. *[3] Assume the family $\{\mathscr{K}_N\}$ of (8) is collectively compact and pointwise convergent on $C(D)$. Let $\{\mathscr{P}_{_N}\}$ be a family of interpolatory projection operators on $C(D)$ to $C(D)$, and assume*

$$\mathscr{P}_{_N}u \longrightarrow u \quad as \quad N \longrightarrow \infty, \tag{24}$$

for all $u \in C(D)$. Finally, assume the integral equation (17) is uniquely solvable for all $h \in C(D)$ and u_* be a unique solution of this equation. Then for all sufficiently large N, say $N \geqslant M$, $(I - \mathscr{K}_N\mathscr{P}_{_N})^{-1}$ exists and is uniformly bounded. Also, for the solution $\bar{u}_N$

$$\|\bar{u}_N - u_*\|_{L^\infty(D)} \leq \|(I - \mathscr{K}_N\mathscr{P}_{_N})^{-1}\|\|\mathscr{K}u_* - \mathscr{K}_N\mathscr{P}_{_N}u_*\|_{L^\infty(D)}. \tag{25}$$

Remark 3. From (24) and the principle of uniform boundedness for the radial basis functions,

$$c_p = \sup\|\mathscr{P}_{_N}\| < \infty. \tag{26}$$

Similarly, from the pointwise convergence of $\{\mathscr{K}_N\}$,

$$c_k = \sup \|\mathscr{K}_N\| < \infty. \tag{27}$$

Theorem 6. *Having in mind the assumptions of (5). Suppose that $u_* \in \aleph_\phi(D)$ is the unique exact solution of equation (5) and the proposed method has been installed on the quasi-uniform set $X = \{(x_i, y_i, z_i)\}_{i=1}^N$. Then there exists $M > 0$ such that for every $N > M$, the method has a unique solution $\hat{u}_N$*

$$\|\hat{u}_N - u_*\|_{L^\infty(D)} \longrightarrow 0 \quad as \quad N \longrightarrow \infty. \tag{28}$$

In addition, for the iterative solution $\bar{u}_N$ for equation (23) we have

$$\|\bar{u}_N - u_*\|_{L^\infty(D)} \leq c_I\{\|\mathscr{K}u_* - \mathscr{K}_N u_*\|_{L^\infty(D)} + c_k(1+c_p)C_l h_{X,D}^l \|u_*\|_{\aleph_\phi(D)}\},$$

provided that $u_* \in \aleph_\phi(D)$, and for the discrete collocation solution $\hat{u}_N$ of equation (20) we have

$$\|\hat{u}_N - u_*\|_{L^\infty(D)} \leq c_p c_I \|\mathscr{K}u_* - \mathscr{K}_N u_*\|_{L^\infty(D)} + (1+c_p)(1+c_p c_I c_k)C_l h_{X,D}^l \|u_*\|_{\aleph_\phi(D)},$$

where $c_I < \infty$ is a bound for $(I - \mathscr{K}_N \mathscr{P}_N)^{-1}$.

Proof. From Theorem 5, the iterated method has a solution $\bar{u}_N$ and

$$\begin{aligned}
\|\bar{u}_N - u_*\|_{L^\infty(D)} &\leq \|(I - \mathscr{K}_N \mathscr{P}_N)^{-1}\| \|\mathscr{K}u_* - \mathscr{K}_N \mathscr{P}_N u_*\|_{L^\infty(D)} \\
&\leq c_I \|\mathscr{K}u_* - \mathscr{K}_N \mathscr{P}_N u_*\|_{L^\infty(D)} \\
&\leq c_I\{\|\mathscr{K}u_* - \mathscr{K}_N u_*\|_{L^\infty(D)} + \|\mathscr{K}_N(u_* - \mathscr{P}_N u_*)\|_{L^\infty(D)}\} \\
&\leq c_I\{\|\mathscr{K}u_* - \mathscr{K}_N u_*\|_{L^\infty(D)} + c_k\|(u_* - \mathscr{P}_N u_*)\|_{L^\infty(D)}\} \\
&\leq c_I\{\|\mathscr{K}u_* - \mathscr{K}_N u_*\|_{L^\infty(D)} + c_k(\|u_* - \hat{u}_*\|_{L^\infty(D)} + \|\mathscr{P}_N u_* - \mathscr{P}_N \hat{u}_*\|_{L^\infty(D)})\} \\
&\leq c_I\{\|\mathscr{K}u_* - \mathscr{K}_N u_*\|_{L^\infty(D)} + c_k(1+c_p)\|(u_* - \hat{u}_*)\|_{L^\infty(D)}\} \\
&\leq c_I\{\|\mathscr{K}u_* - \mathscr{K}_N u_*\|_{L^\infty(D)} + c_k(1+c_p)C_l h_{X,D}^l \|u_*\|_{\aleph_\phi(D)}\}
\end{aligned}$$

The last inequality is implied by (15). Moreover, let $\hat{u}_N = p_N \bar{u}_N$, and consider the decomposition

$$u_* - \hat{u}_N = u_* - \mathscr{P}_N \bar{u}_N = (u_* - \mathscr{P}_N u_*) + \mathscr{P}_N(u_* - \bar{u}_N), \tag{29}$$

which yields

$$\begin{aligned}\|\hat{u}_N - u_*\|_{L^\infty(D)} &\leq \|u_* - \mathscr{P}_N u_*\|_{L^\infty(D)} + c_p\|\bar{u}_N - u_*\|_{L^\infty(D)} \\ &\leq (1+c_p)C_l h^l_{X,D}|u_*|_{\aleph_\phi(D)} + c_p(c_I\{\|\mathscr{K}u_* - \mathscr{K}_N u_*\|_{L^\infty(D)} \\ &\quad + c_k(1+c_p)C_l h^l_{X,D}|u_*|_{\aleph_\phi(D)}\}) \\ &\leq \underbrace{c_p c_I\|\mathscr{K}u_* - \mathscr{K}_N u_*\|_{L^\infty(D)}}_{N\longrightarrow\infty \implies \mathscr{K}_N\longrightarrow\mathscr{K}} \\ &\quad + \underbrace{(1+c_p)(1+c_p c_I c_k)C_l h^l_{X,D}\|u_*\|_{\aleph_\phi(D)}}_{N\longrightarrow\infty \implies h_{X,D}\longrightarrow 0}\end{aligned}$$

Finally, we obtain

$$\|\hat{u}_N - u_*\|_{L^\infty(D)} \longrightarrow 0 \quad as \quad N \longrightarrow \infty.$$

Corollary 1. *Theorem 6 shows that, both the quadrature and the RBF approximation error bounds affect the final estimation. If for a sufficiently smooth kernel $K(x,t,y,s)$ a high order quadrature is employed then the total error is dominated by the error of the RBF approximation.*

5 Numerical examples

In this section, we present some numerical examples where D is a bounded domain in $\mathbb{R}^3$. In addition to the Hardy, Franke and Fasshauer shape parameters, the minimum error obtained by trial and error is presented. We have used the ten-point Gauss-Legendre quadrature rule for numerical integration. All of the computations have been done using the Maple 14 with just 80 digits precision. we calculate the RMS error in 2197 points that are distributed uniformly in the computational domain. The RMS error of the numerical result is described using

$$RMS = \sqrt{\frac{1}{2197}\sum_{i=1}^{2197} \mid u(x_i,y_i,z_i) - \hat{u}(x_i,y_i,z_i) \mid^2}$$

where $u(x,y,z)$ is the exact solution, $\hat{u}(x,y,z)$ is the approximate solution.

Example 1. Consider the three-dimensional linear Fredholm integral equation

$$u(x,y,z) - \frac{1}{2}\int_{-1}^{1}\int_{-1}^{1}\int_{-1}^{1}\frac{xyz}{1+x+y+z}u(r,s,t)drdsdt = f(x,y,z),$$

where

$$f(x,y,z) = \sin^2(x)\sin^2(y)\sin^2(z) + \big(\cos(1)\sin(1) - 1\big)^3 \frac{xyz}{2 + 2x + 2y + 2z}.$$

The exact solution for this equation is $u(x,y,z) = \sin^2(x)\sin^2(y)\sin^2(z)$.

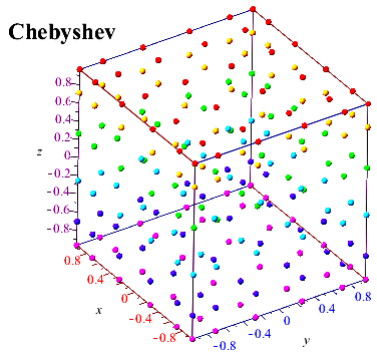

Figure 3: Node distribution with 216 nodes for Example 1.

The results obtained by the Chebyshev distribution of points for different numbers of N in terms of RMS is given in Tables 2, 3 and 4. The distribution of nodes are depicted for N = 216 in Figure 3. As we expected, from Theorem 6, the results converge to the exact values along with the increase of the nodes. In computations, for GA RBFs, to obtain the better result, we can use the small(big) parameter c but the condition number of the final system is grown fast instead. As can be seen, the convergence rate of the method is arbitrarily high when GAs and IQs are used and is approximately $O(h^k_{X,D})$ when TPSs and CSs are used. Therefore the numerical results confirm the theoretical error estimates.

Example 2. Consider the three-dimensional linear Fredholm integral equation

$$u(x,y,z) - \frac{1}{2}\int_0^2 \int_0^1 \int_{-1}^1 \sin(xyz)u(r,s,t)drdsdt = f(x,y,z),$$

where

$$f(x,y,z) = x^2y^2z^2 - \frac{8}{27}\sin(xyz),$$

with exact solution $u(x,y,z) = x^2y^2z^2$. The results obtained by the Regular distribution of points for different numbers of N in terms of RMS is given in Tables 5, 6 and 7. The distribution of nodes are depicted for N = 294 in Figure 4. It should be noted that for a fixed sufficiently large m_N, by increasing N, the error of the method is of $O(h^l_{X,D})$ (i.e., arbitrarily high for the use of MQs and IMQs and approximately $O(h^k_{X,D})$ for the use of

Table 2: Results provided by Chebyshev distribution for Example 1.

N	$h_{X,D}$	*shape parameter*	c	GA
27	0.7339	$Hardy$	0.70	7.36×10^{-2}
		$Franke$	0.72	8.13×10^{-2}
		$Fasshauer$	0.38	2.52×10^{-4}
		a^*	0.38	2.52×10^{-4}
64	0.6334	$Hardy$	0.44	7.88×10^{-4}
		$Franke$	0.50	1.59×10^{-3}
		$Fasshauer$	0.25	4.83×10^{-3}
		a^*	0.43	7.75×10^{-4}
125	0.4991	$Hardy$	0.30	2.11×10^{-4}
		$Franke$	0.37	2.51×10^{-4}
		$Fasshauer$	0.18	7.50×10^{-5}
		a^*	0.20	4.24×10^{-6}
216	0.4189	$Hardy$	0.22	5.13×10^{-5}
		$Franke$	0.28	2.02×10^{-4}
		$Fasshauer$	0.14	2.35×10^{-4}
		a^*	0.20	2.20×10^{-6}

a^* indicates the shape parameter which minimum error is observed.

Table 3: Results provided by Chebyshev distribution for Example 1.

N	$h_{X,D}$	CS		TPS	
		$k=1$	$k=2$	$k=1$	$k=2$
27	0.7339	9.14×10^{-2}	3.92×10^{-2}	1.56×10^{-1}	2.21×10^{-1}
64	0.6334	3.36×10^{-2}	1.71×10^{-2}	5.88×10^{-2}	4.82×10^{-2}
125	0.4991	2.29×10^{-2}	5.76×10^{-3}	1.17×10^{-2}	4.54×10^{-3}
216	0.4189	1.71×10^{-2}	3.34×10^{-3}	6.05×10^{-3}	2.64×10^{-3}

Table 4: Results provided by Chebyshev distribution for Example 1.

N	$h_{X,D}$	*shape parameter*	c	IQ
27	0.7339	$Hardy$	0.70	2.24×10^{-2}
		$Franke$	0.72	2.29×10^{-2}
		$Fasshauer$	0.38	3.52×10^{-2}
		a^*	1.25	1.57×10^{-3}
64	0.6334	$Hardy$	0.44	7.44×10^{-3}
		$Franke$	0.50	6.27×10^{-3}
		$Fasshauer$	0.25	9.30×10^{-3}
		a^*	0.93	8.91×10^{-4}
125	0.4991	$Hardy$	0.30	6.60×10^{-3}
		$Franke$	0.37	4.82×10^{-3}
		$Fasshauer$	0.18	8.22×10^{-3}
		a^*	1.61	1.43×10^{-4}
216	0.4189	$Hardy$	0.22	4.34×10^{-3}
		$Franke$	0.28	2.35×10^{-3}
		$Fasshauer$	0.14	6.23×10^{-3}
		a^*	0.92	7.84×10^{-5}

a^* indicates the shape parameter which minimum error is observed.

TPSs and CSs) because the RBF interpolation error overcomes the error of integration method and so increasing N has no significant effect on the error. Based on the obtained fill distance, the results confirm Theorem 6.

Example 3. Consider the three-dimensional linear Fredholm integral equation

$$u(x,y,z) - \frac{1}{2}\int_0^1\int_0^1\int_0^1 xyzu(r,s,t)drdsdt = f(x,y,z),$$

where

$$f(x,y,z) = xyz\exp(-x^2-y^2-z^2) - \frac{1}{16}\left(1-\frac{1}{\exp(1)}\right)^3 xyz,$$

with exact solution $u(x,y,z) = xyz\exp(-x^2-y^2-z^2)$. The results obtained by the Halton distribution of points for different numbers of N in terms of RMS is given in Tables 8, 9 and 10. A set of 216 Halton points in the unit cubic in $\mathbb{R}^3$ has been shown in Figure 5. For sufficiently large m_N, increasing

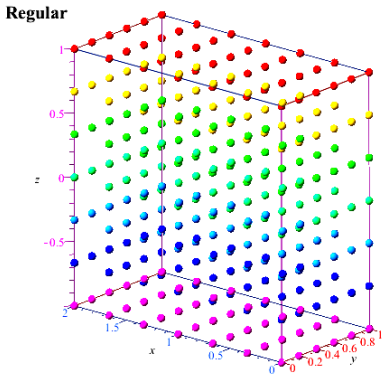

Figure 4: Node distribution with 294 nodes for Example 2.

Table 5: Results provided by Regular distribution for Example 2.

N	$h_{X,D}$	*shape parameter*	c	MQ
48	0.5246	*Hardy*	0.41	1.01×10^{-2}
		Franke	0.54	9.82×10^{-3}
		Fasshauer	0.29	1.12×10^{-2}
		a^*	1.82	7.21×10^{-3}
100	0.3842	*Hardy*	0.27	5.16×10^{-3}
		Franke	0.37	4.81×10^{-3}
		Fasshauer	0.20	5.26×10^{-3}
		a^*	4.23	9.39×10^{-4}
180	0.3039	*Hardy*	0.20	3.26×10^{-3}
		Franke	0.28	3.09×10^{-3}
		Fasshauer	0.15	3.30×10^{-3}
		a^*	5.54	2.20×10^{-4}
294	0.2517	*Hardy*	0.16	2.16×10^{-3}
		Franke	0.22	2.04×10^{-3}
		Fasshauer	0.12	2.19×10^{-3}
		a^*	5.52	3.88×10^{-5}

a^* indicates the shape parameter which minimum error is observed.

the number of integration nodes m_N has no significant effect on the error and the proposed method will be of $O(h^l_{X,D})$, by increasing N. The numerical

Table 6: Results provided by Regular distribution for Example 2.

N	$h_{X,D}$	*shape parameter*	c	IMQ
48	0.5246	$Hardy$	0.41	1.35×10^{-2}
		$Franke$	0.54	1.39×10^{-2}
		$Fasshauer$	0.29	1.20×10^{-2}
		a^*	2.79	4.72×10^{-3}
100	0.3842	$Hardy$	0.27	7.23×10^{-3}
		$Franke$	0.37	7.73×10^{-3}
		$Fasshauer$	0.20	6.32×10^{-3}
		a^*	4.71	6.68×10^{-4}
180	0.3039	$Hardy$	0.20	4.51×10^{-3}
		$Franke$	0.28	5.08×10^{-3}
		$Fasshauer$	0.15	4.11×10^{-3}
		a^*	8.40	8.02×10^{-5}
294	0.2517	$Hardy$	0.16	3.07×10^{-3}
		$Franke$	0.22	3.51×10^{-3}
		$Fasshauer$	0.12	3.13×10^{-3}
		a^*	5.52	3.88×10^{-5}

a^* indicates the shape parameter which minimum error is observed.

Table 7: Results provided by Regular distribution for Example 2.

N	$h_{X,D}$	CS		TPS	
		$k=1$	$k=2$	$k=1$	$k=2$
48	0.5246	9.92×10^{-2}	8.70×10^{-2}	1.05×10^{-1}	1.00×10^{-1}
100	0.3842	4.87×10^{-2}	3.76×10^{-2}	4.63×10^{-2}	3.15×10^{-2}
180	0.3039	3.18×10^{-2}	2.06×10^{-2}	2.71×10^{-2}	1.53×10^{-2}
294	0.2517	2.22×10^{-2}	1.16×10^{-2}	1.69×10^{-2}	7.76×10^{-3}

results confirm the theoretical error estimates. In addition, the numerical results shows that the accuracy of RBFs with shape parameter is better than RBFs without shape parameter.

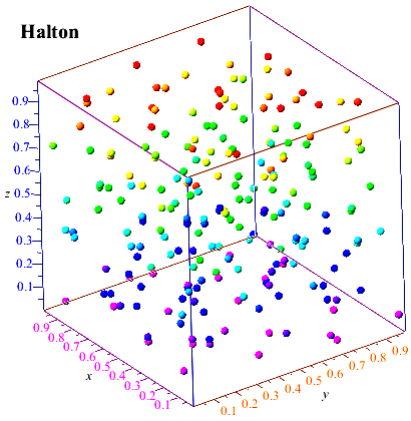

Figure 5: Node distribution with 216 nodes for Example 3.

6 Conclusion

In this paper, a collocation method based on RBFs for numerical solution of three-dimensional linear Fredholm integral equations of the second kind on the cubic domains is presented. The proposed method is a meshless method, which requires no domain elements for the interpolation or approximation. The Gauss-Legendre quadrature formula is employed for numerical integration. Error analysis was provided for suffficiently smooth kernel and source functions. The method is very convenient for solving higher dimensional integral equations because the RBF is defined as the function of distance. The proposed method can be easily expanded into non-cube domains. It means the process of solving is no more complicated in spite of increasing the dimension of problem. This is significant advantage of the method in comparision with other strategy for solving Integral Equations in three dimension.

Acknowledgements

Authors are grateful to there anonymous referees and editor for their constructive comments.

Table 8: Results provided by Halton distribution for Example 3.

N	$h_{X,D}$	*shape parameter*	c	GA
27	0.4912	$Hardy$	0.22	4.16×10^{-3}
		$Franke$	0.29	3.88×10^{-3}
		$Fasshauer$	0.38	3.56×10^{-3}
		a^*	1.57	1.81×10^{-3}
64	0.3456	$Hardy$	0.14	9.10×10^{-4}
		$Franke$	0.20	7.84×10^{-4}
		$Fasshauer$	0.25	6.89×10^{-4}
		a^*	0.88	8.57×10^{-5}
125	0.2820	$Hardy$	0.12	1.76×10^{-4}
		$Franke$	0.17	1.51×10^{-4}
		$Fasshauer$	0.18	1.46×10^{-4}
		a^*	0.84	7.45×10^{-6}
216	0.2780	$Hardy$	0.09	2.14×10^{-5}
		$Franke$	0.13	1.70×10^{-5}
		$Fasshauer$	0.14	1.61×10^{-5}
		a^*	0.90	9.10×10^{-8}

a^* indicates the shape parameter which minimum error is observed.

Table 9: Results provided by Halton distribution for Example 3.

N	$h_{X,D}$	CS		TPS	
		$k=1$	$k=2$	$k=1$	$k=2$
27	0.4912	5.34×10^{-2}	1.09×10^{-2}	2.12×10^{-2}	4.07×10^{-2}
64	0.3456	3.61×10^{-3}	3.22×10^{-3}	1.47×10^{-2}	5.90×10^{-3}
125	0.2820	2.28×10^{-3}	1.60×10^{-3}	9.15×10^{-3}	3.43×10^{-3}
216	0.2780	1.74×10^{-3}	4.88×10^{-4}	2.04×10^{-3}	1.35×10^{-3}

Table 10: Results provided by Halton distribution for Example 3.

N	$h_{X,D}$	*shape parameter*	c	MQ
27	0.4912	$Hardy$	0.22	3.91×10^{-3}
		$Franke$	0.29	3.77×10^{-3}
		$Fasshauer$	0.38	3.65×10^{-3}
		a^*	1.60	2.95×10^{-3}
64	0.3456	$Hardy$	0.14	2.38×10^{-3}
		$Franke$	0.20	2.14×10^{-3}
		$Fasshauer$	0.25	1.99×10^{-3}
		a^*	1.80	2.06×10^{-4}
125	0.2820	$Hardy$	0.12	1.64×10^{-3}
		$Franke$	0.17	1.46×10^{-3}
		$Fasshauer$	0.18	1.43×10^{-3}
		a^*	2.60	1.74×10^{-5}
216	0.2780	$Hardy$	0.09	1.20×10^{-3}
		$Franke$	0.13	1.02×10^{-3}
		$Fasshauer$	0.14	9.73×10^{-4}
		a^*	2.10	1.46×10^{-6}

a^* indicates the shape parameter which minimum error is observed.

References

1. Alipanah, A. and Esmaeili, S. *Numerical solution of the two-dimensional Fredholm integral equations using Gaussian radial basis function*, J. Comput. Appl. Math. 235 (2011), 5342-5347.

2. Assari, P., Adibi, H. and Dehghan, M. *A numerical method for solving linear integral equations of the second kind on the non-rectangular domains based on the meshless method*, Applied Mathematical Modelling, 37 (2013), 9269-9294.

3. Atkinson, K.E. *The Numerical Solution of Integral Equations of the Second Kind*, vol. 4, Cambridge University Press, Cambridge, UK, 1997.

4. Atkinson, K.E. and Han, W. *Theoretical Numerical Analysis: a Functional Analysis Framework*, Springer-Verlag New York, INC, 2001.

5. Brunner, H. *Collocation Methods for Volterra Integral and Related Functional Equations*, Cambridge University Press, 2004.

6. Dehghan, M. and Mirzaei, D. *Meshless Local Petrov-Galerkin (MLPG) method for the unsteady magnetohydrodynamic (MHD) flow through pipe with arbitrary wall conductivity*, App. Numer. Math. 59 (2009), 1043-1058.

7. Dehghan, M. and Salehi, R. *The numerical solution of the non-linear integro-differential equations based on the meshless method*, J. Comput. Appl. Math. 236 (2012), 2367-2377 .

8. Fasshauer, G. E. *Meshfree approximation methods with MATLAB*, Interdisciplinary Mathematical Sciences, vol. 6. World Scientific Publishing Company, Singapore, 2007.

9. Fasshauer, G.E. *Newton iteration with multiquadrics for the solution of nonlinear PDEs*, Computers and Mathematics with Applications, 43 (2002), 423-438.

10. Franke, R. *Scattered data interpolation: Tests of some methods*, Mathematics of Computation, 38 (1982), 181-200.

11. Golbabai, A., Mammadov, M. and Seifollahi, S. *Solving a system of nonlinear integral equations by an RBF network*, Comput. Math. Appl. 57 (2009), 1651-1658.

12. Golbabai, A. and Seifollahi, S. *Numerical solution of the second kind integral equations using radial basis function networks*, Appl. Math. Comput. 174 (2006), 877-883.

13. Golbabai, A. and Seifollahi, S. *Radial basis function networks in the numerical solution of linear integro-differential equations*, Appl. Math. Comput. 188 (2007), 427-432.

14. Guoqiang, H., Hayami, K., Sugihara,K. and Jiong, W. *Extrapolation method of iterated collocation solution for two-dimensional nonlinear Volterra integral equations*, Appl. Math. Comput. 112 (2000), 49-61.

15. Guoqiang, H. and Jiong, W. *Extrapolation of nystrom solution for two dimensional nonlinear Fredholm integral equations*, J. Comput. Appl. Math. 134 (2001), 259-268.

16. Hardy, R. L. *Multiquadric equations of topography and other irregular surfaces*, J. Geophys. Res. 176 (1971), 1905-1915.

17. Hon, Y.C., Cheung, K.F., Mao, X.Z. and Kansa, E.J. *Multiquadric solution for shallow water equations*, ASCE J. Hydraul. Eng. 125 (5) (1999), 524-533.

18. Hon, Y.C. and Mao, X.Z. *An efficient numerical scheme for Burgers equation*, Appl. Math. Comput. 95 (1) (1998), 37-50.

19. Hon, Y.C. and Mao, X.Z. *A radial basis function method for solving options pricing model*, Financ. Eng. 8 (1) (1999), 31-49.

20. Kansa, E.J. *Multiquadrics - A scattered data approximation scheme with applications to computational fluid dynamics-I*, Comput. Math. Appl. 19 (1990), 127-145.

21. Kansa, E.J. *Multiquadrics - A scattered data approximation scheme with applications to computational fluid dynamics-II*, Comput. Math. Appl. 19 (1990), 147-161.

22. Larsson, E. and Fornberg, B. *A numerical study of some radial basis function based solution methods for elliptic PDEs*, Comput. Math. Appl. 46 (2003), 891-902.

23. Marcozzi, M., Choi, S. and Chen, C.S. *On the use of boundary conditions for variational formulations arising in financial mathematics*, Appl. Math. Comput. 124 (2001), 197-214.

24. Micchelli, C.A. *Interpolation of scattered data: distance matrices and conditionally positive denite functions*, Constr. Approx., 2 (1986), 11-22.

25. Parand, K. and Rad, J.A. *Numerical solution of nonlinear Volterra-Fredholm-Hammerstein integral equations via collocation method based on radial basis functions*, Appl. Math. Comput. 218 (2012), 5292-5309.

26. Salehi, R. and Dehghan, M. *A moving least square reproducing polynomial meshless method*, Appl. Numer. Math. 69 (2013), 34-58.

27. Schoenberg, I. J. *Metric spaces and completely monotone functions*, Ann. Math., 39 (1938), 811-841.

28. Wendland, H. *Scattered data approximation*, Cambridge Monographs on Applied and Computational Mathematics, vol. 17. Cambridge University Press, Cambridge 2005.

29. Xie, W. J. and Lin, F. R. *A fast numerical solution method for two dimensional Fredholm integral equations of the second kind*, Applied Numerical Mathematics, 59 (2009), 1709-1719.

30. Zerroukat, M., Power, H. and Chen, C.S. *A numerical method for heat transfer problem using collocation and radial basis functions*, Internat. J. Numer. Methods Engrg. 42 (1992), 1263-1278.

روش توابع پایه شعاعی برای حل معادلات انتگرال فردهلم خطی سه بعدی روی دامنه های مکعبی

محسن اسماعیل بیگی، فرشید میرزایی و داود معظمی

دانشگاه ملایر، دانشکده علوم ریاضی و آمار، گروه ریاضی

دریافت مقاله ۱۸ آذر ۱۳۹۴، دریافت مقاله اصلاح شده ۱۴ شهریور ۱۳۹۵، پذیرش مقاله ۲۶ آبان ۱۳۹۵

چکیده : هدف اصلی این مقاله ارایه یک روش عددی کارآمد برای حل معادلات انتگرال فردهلم خطی از نوع دوم روی دامنه های سه بعدی مکعبی می باشد. روش ارایه شده بر اساس درونیاب توابع پایه شعاعی مبتنی بر نقاط و وزنهای گاوس لژاندر طراحی شده است. آنالیز خطا برای روش مدنظر بیان شده است. به کمک مثالهای عددی متنوع قابلیت و کارایی روش، مورد سنجش و ارزیابی قرار گرفته است.

کلمات کلیدی : معادلات انتگرال سه بعدی؛ توابع پایه شعاعی؛ روش هم محلی؛ دامنه های مکعبی.